International Journal of Mass Spectrometry and Ion Physics, 18 (1975) 1–9

EFFECT OF ION ENTRY PHASE, RADIAL VELOCITY AND POSITION ON QUADRUPOLE MASS FILTER OPERATION

P. K. GHOSH, ABHA JAIN AND R. NAGARAJAN*
Department of Chemistry, Indian Institute of Technology, Kanpur 208016 (India)
(First received 2 October 1974; in final form 3 January 1975)

ABSTRACT

The effect of the ion entry conditions on quadrupole mass filter operation in terms of resolution–ion transmission characteristics has been studied by numerical calculations of ion trajectories for various sets of ion injection velocity, position and phase. The conventional "stability diagram" on the a–q plane describing the parametric region of stable solutions of Mathieu's equation is contrasted with "practical stability diagrams" describing the parametric regions of "bounded" solutions of Mathieu's equation. It is shown that if the initial radial velocity–position–phase injection conditions are specified, the mass filter can be operated at high resolution using constant a/q lines other than that required for the apex region of the conventional stability diagram. An extension of the definition of resolution has been proposed to apply to specific initial ion injection conditions.

INTRODUCTION

The stability diagram obtained from the qualitative (i.e., without explicit calculations of $x(t)$ and $y(t)$) solution of Mathieu's equation is generally used [1] to understand the operation of the quadrupole mass filter using hyperbolic electrode surfaces. The innate stability or instability of ions described by the stable and unstable regions in the a–q parameter space is independent of the initial conditions of entry of the ions and is solely determined by the values of the parameters a and q. But whether or not an injected ion will be transmitted through a field of finite dimensions is determined by the initial conditions of ion entry. Two cases arise: (1) where the ion is inherently unstable but is transmitted through the field

* Present address: Department of Chemical Engineering, State University of New York at Buffalo, N.Y., U.S.A.

as its amplitude of oscillation remains bounded and is less than the field dimension for the finite number of r.f. cycles it experiences, and (2) when the inherently stable ion is lost to the electrode surface because the amplitude of its oscillations, though finite, exceeds the bound imposed by the finite field dimension. So, for practical mass spectrometer operations, it is necessary to locate the parametric region corresponding to bounded ion trajectories for given initial conditions of radial velocity, position and phase of injection. Such "practical stability diagrams" representing regions of bounded ion oscillations, have the potential to explain the transmission behaviour of a sample of ions where the entry conditions are of a particular distribution.

To realize this objective, ion trajectories first need to be studied for a wide range of initial conditions of position and velocity as well as of phase. In preliminary work [2], we studied ion trajectories for several combinations of position and radial velocities at *zero* initial phase and attempted to relate empirically the location of practical stability diagram peaks to the initial conditions through resolution, as commonly defined [1, 3]. In a practical instrument, however, injection ordinarily takes place continuously for all phases, and trajectory information is needed accordingly. Such information, when available, can be used, with appropriate averaging, to predict resolution and peak shape in an actual spectrum. In the present paper we report the results of our investigation of the effect of varying the initial phase on resolution–ion transmission characteristics and discuss the effects of a constant a/q ratio line on mass filter resolution for specific initial conditions of ion injection.

ION TRAJECTORY COMPUTATIONS

The motion of ions in a two-dimensional quadrupole field is described by the differential equations

$$\frac{d^2x}{d\xi^2}+(a+2q\cos 2\xi)x = 0$$

$$\frac{d^2y}{d\xi^2}-(a+2q\cos 2\xi)y = 0$$

where $a = 8eU/mr_0^2\omega^2$, $q = 4eV/mr_0^2\omega^2$ and $\xi = \omega t/2$; m and e are respectively the ionic mass and the charge, U the d.c. component and V the peak r.f. (angular frequency ω) amplitude of the potential on the electrodes, the closest distance between the opposite electrodes being $2r_0$. The method of ion trajectory computation using numerical integration of Mathieu's equation with specific initial conditions has already been described [2]. Various a, q operation points in the range $q = 0.699$–0.708 were chosen along mass scan lines with resolutions

$m/\Delta m$ = 100–1000 (as defined in refs. 1, 3) and ion trajectories were computed for about 160 cycles of ion motion. From the maxima of the trajectories, limiting lines were obtained on the a, q diagram which show the domain of a, q values for which the ion amplitudes remain bounded, i.e., both x and y remain less than r_0. Since the x and y equations of motion are independent of one another, various practical stability diagrams were obtained for different combinations of x_0, x_0', y_0, y_0' and ξ_0.

The present computations involve eight sets of initial position–velocity conditions, x_0 (or y_0), x_0' (or y_0') being (in length and length/radian respectively) 0.015, 0.012; 0.010, 0.015; 0.012, 0.010; 0.010, 0.010; 0.015, 0.005; 0.005, 0.010; 0.008, 0.008; 0.010, 0.005; and each such condition for a set of 8 initial phases at entry in the range of $\xi_0 = 0$ to π, in steps of $\pi/8$.

RESULTS

The results of trajectory computations, in the form of the a, q value of apex points of the practical stability diagrams, are given in Table I for the eight sets of initial radial velocity–position and eight initial phases. A set of typical practical stability diagrams is shown in Fig. 1 describing the parametric space of bounded oscillations for the initial phase $\xi_0 = 3\pi/8$. The effect of initial phase variation

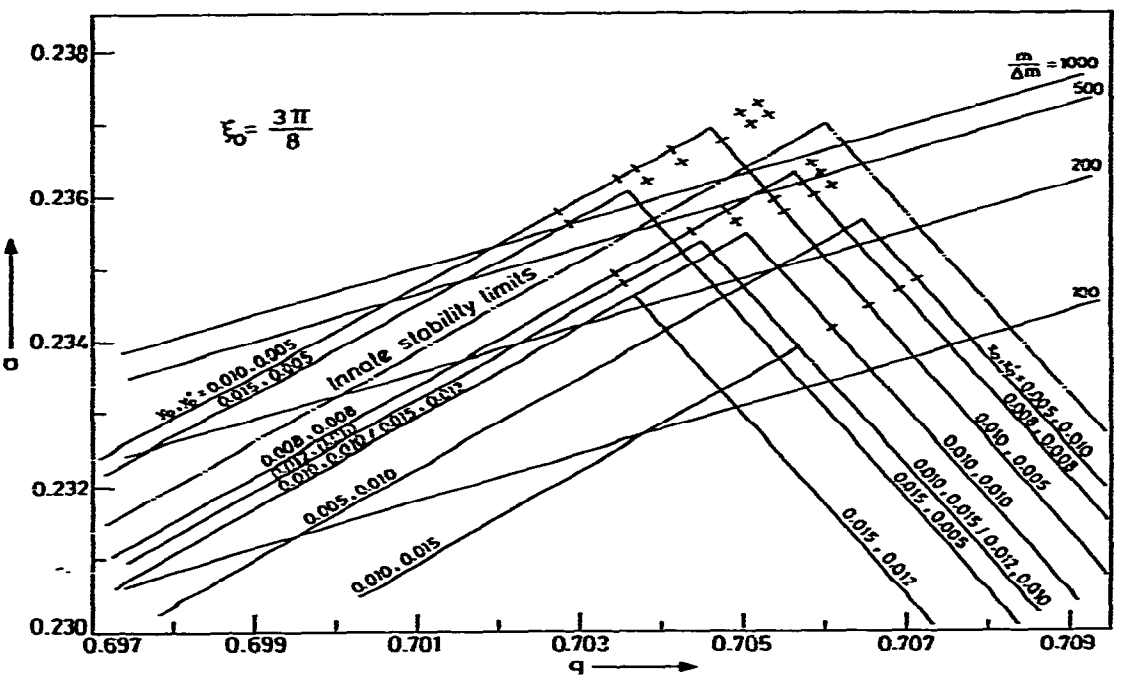

Fig. 1. Practical stability diagrams for $\xi_0 = 3\pi/8$.

TABLE I

PRACTICAL STABILITY DIAGRAM APEX POINTS[a]

$\xi_0 = 0$

	1	2	3	4	5	6	7	8
1	0.23505	470	535	530	585	535	560	575
	0.70485	510	465	465	420	465	440	430
2	440	410	470	465	520	470	495	510
	380	410	360	360	320	360	340	325
3	535	500	565	560	615	565	590	605
	535	560	510	515	470	510	490	475
4	555	520	580	580	635	580	610	625
	560	590	540	545	500	540	520	510
5	610	575	635	630	690	635	660	680
	650	675	630	630	585	630	610	595
6	540	510	570	565	620	570	595	610
	545	570	520	525	480	520	500	485
7	570	535	600	595	650	600	625	640
	590	615	565	570	525	565	545	530
8	610	575	635	630	690	635	660	680
	650	675	630	630	585	630	610	595

$\xi_0 = \pi/8$

	1	2	3	4	5	6	7	8
1	405	340	415	395	425	370	405	
	130	180	120	135	110	160	130	
2	415	350	420	405	435	380	415	
	145	195	135	150	130	170	145	
3	505	445	515	500	530	475	505	
	295	340	285	300	275	320	295	
4	530	470	540	525	550	495	530	
	335	380	325	340	315	360	335	
5	555	495	565	550	575	520	555	
	370	420	365	380	355	400	370	
6	585	525	595	580	610	555	585	
	420	470	415	430	405	450	420	
7	620	555	630	610	640	585	620	
	470	520	465	480	455	495	470	
8	620	555	630	610	640	585	620	
	470	520	465	480	455	495	470	

$\xi_0 = \pi/4$

	1	2	3	4	5	6	7	8
	430	330	430	405	380	360	415	450
	110	195	110	135	155	170	120	095
	495	395	495	470	445	425	480	515
	215	295	215	235	255	275	225	200
	530	430	530	505	475	455	515	550
	270	350	270	290	310	325	280	255
	580	475	580	550	525	500	560	595
	340	425	340	365	385	400	355	330
	550	450	550	525	495	475	535	570
	300	380	300	320	340	360	310	285
	655	555	655	630	600	580	640	675
	470	550	470	490	510	530	480	455
	645	540	645	620	590	570	630	660
	450	530	450	470	490	510	460	435
	630	525	630	605	575	555	615	650
	425	510	425	450	470	485	440	415

$\xi_0 = 3\pi/8$

	1	2	3	4	5	6	7	8
1	460	330	480	460	565	415	490	580
	365	470	350	365	285	405	390	270
2	520	390	535	520	620	475	550	635
	460	565	450	460	380	500	435	365
3	520	390	535	520	620	475	550	635
	460	565	450	460	380	500	435	365
4	550	415	565	550	645	500	580	665
	505	610	490	505	425	540	475	410
5	510	375	525	510	605	460	535	625
	440	545	425	440	355	475	415	345
6	615	485	630	615	710	565	645	725
	605	715	595	605	525	645	580	515

$\xi_0 = \pi/2$

405	405	555	405	495	555	
615	615	495	615	545	495	
465	465	610	465	355	610	
705	705	590	705	635	590	
445	445	590	445	530	590	
670	670	555	670	600	555	
475	475	620	475	560	620	
720	720	605	720	650	605	
425	425	575	425	515	575	
645	645	530	645	575	530	
520	520	665	520	605	665	
790	790	675	790	720	675	

TABLE I (continued)

7	600	470	615	600	700	555	630	715			485	485	630	485	570	630
	585	690	575	585	505	625	560	495			735	735	620	735	665	620
8	580	445	595	580	675	530	610	690			465	465	610	465	550	610
	550	655	535	550	470	585	525	460			705	705	590	705	635	590

$\xi_0 = 5\pi/8$

	1	2	3	4	5	6	7	8
1					430	395	465	505
					705	730	680	645
2					515	480	550	590
					835	865	810	780
3					450	415	480	525
					730	760	705	670
4					470	420	505	550
					770	795	745	710
5					400	365	435	475
					655	685	630	595
6					560	530	595	640
					915	940	890	855
7					495	460	530	575
					805	835	780	730
8					460	430	495	540
					755	780	730	695

$\xi_0 = 3\pi/4$

	1	2	3	4	5	6	7	8
1					425	490	520	530
					780	730	710	695
2								
3					460	525	550	565
					830	780	760	745
4					490	550	580	595
					880	830	805	795
5					380	445	470	490
					710	660	635	625
6					515	580	605	625
					920	870	850	840
7					525	590	620	630
					940	885	860	850
8					425	490	520	530
					780	730	710	695

$\xi_0 = 7\pi/8$

	1	2	3	4	5	6	7	8
1	525	515	605	630	670	680	700	705
	945	950	880	860	825	815	800	795
2	395	385	475	500	540	555	575	580
	745	750	680	660	625	620	600	595
3	525	515	605	630	670	680	700	705
	945	950	880	860	825	815	800	795
4	480	475	560	585	625	635	655	665
	880	880	815	795	760	750	735	730
5	430	425	510	540	580	590	610	620
	805	810	740	740	685	680	660	655
6	420	415	500	525	570	580	600	610
	785	790	725	705	670	660	645	640
7	505	500	585	610	650	660	685	690
	915	920	855	835	800	790	775	770
8	520	510	595	620	660	670	690	700
	935	940	870	850	815	805	790	785

$\xi_0 = \pi$

	1	2	3	4	5	6	7	8
1	500	460	520	515	575	530	550	575
	460	495	445	450	400	440	425	400
2	440	400	465	455	515	470	490	515
	370	405	355	360	310	350	330	310
3	550	510	570	565	625	580	600	625
	545	575	530	535	485	520	505	485
4	545	505	570	560	620	575	595	620
	535	570	520	525	475	515	495	475
5	610	570	635	625	685	640	660	685
	640	670	620	625	580	615	600	580
6	550	510	570	565	625	580	600	625
	545	575	530	535	485	520	505	485
7	585	545	605	600	660	610	630	660
	595	630	580	585	535	575	560	535
8	610	570	635	625	685	640	660	685
	640	670	620	625	580	615	600	580

[a] The a, q values of the apex points are reported (estimated error ± 0.0001) as a function of the initial conditions. Each section of the Table is for a specific ξ_0, wherein the rows and columns represent (x_0, x_0') and (y_0, y_0') respectively. For numerical values of x_0, x_0' or y_0, y_0', the following notations are used: (1) 0.015, 0.012; (2) 0.010, 0.015; (3) 0.012, 0.010; (4) 0.010, 0.010; (5) 0.015, 0.005; (6) 0.005, 0.010; (7) 0.008, 0.008; (8) 0.010, 0.005. Several x, y limit lines could not be plotted as the corresponding x (or y) amplitudes are either too small or too large for intersection with the $r_0/x_0, y_0$ limiting line. $\pi/8$: 0.010, 0.005 y amplitudes are too small. $\pi/2$: 0.010, 0.015 and 0.015, 0.012 y amplitudes are too large. $5\pi/8$: 0.010, 0.015; 0.010, 0.010; 0.012, 0.010 and 0.015, 0.012 y amplitudes are too large. $3\pi/4$: 0.010, 0.015 x amplitudes are too small and y amplitudes are too large; also, for 0.015, 0.012; 0.012, 0.010; 0.010, 0.010 y amplitudes are too large.

on the location of the apex point for a given set of initial velocity–position conditions is illustrated in Fig. 2 using the initial conditions x_0, x_0', y_0, y_0' of 0.008, 0.008, 0.008, 0.008 and 0.010, 0.010, 0.008, 0.008 respectively and about sixteen ξ_0 values.

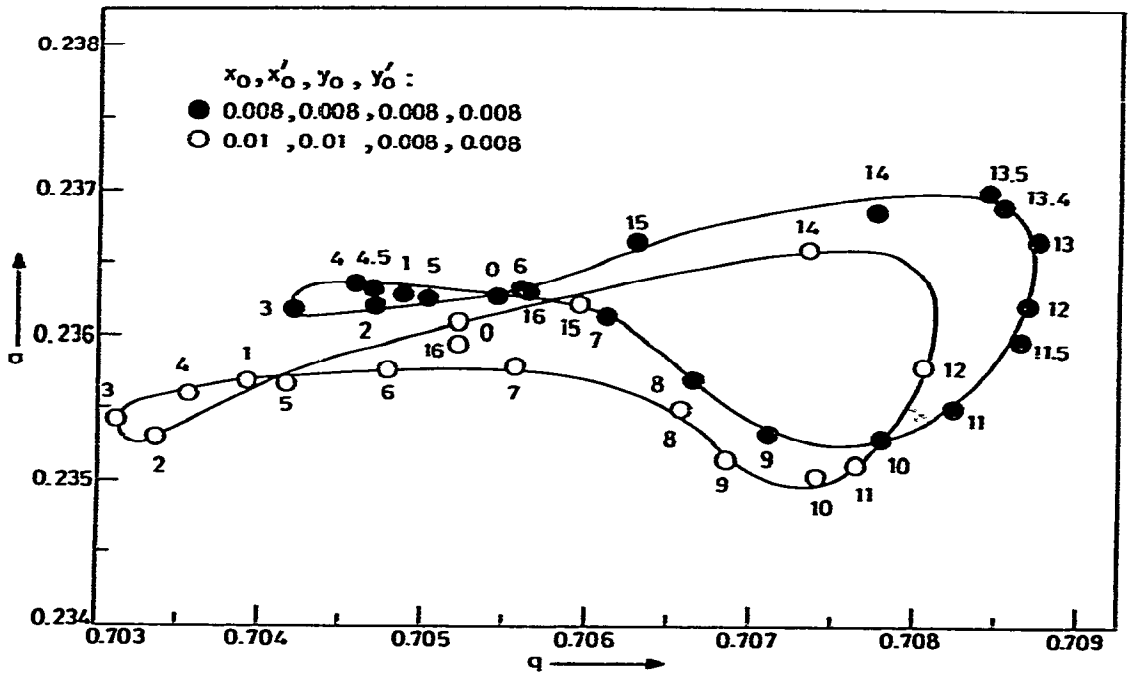

Fig. 2. Practical stability diagram apex point loci due to initial phase ξ_0 variation. The circles represent apex points from actual computation for specific initial phases; the ξ_0 values are shown next to the circles in units of $\pi/16$. The locus between the open circles for $\xi_0 = 12(\pi/16)$ and $\xi_0 = 14(\pi/16)$, in the absence of information on $13(\pi/16)$, is somewhat uncertain.

Errors arise in finding the intersection of the x_m/x_0, y_m/y_0 versus q curves with the r_0/x_0, y_0 limiting line (r_0 is taken as 0.350) as well as in drawing the x, y limiting lines of practical stability diagrams. We estimate the overall error in the reported a, q points at the x–y limit intersections as less than ± 0.0001 for both a and q. Within this error margin the x, y limit lines of the practical stability diagrams are essentially parallel to the x, y limit lines of the conventional stability diagram. In plotting the limit lines of the former, more weight was given to those x_m/x_0, y_m/y_0 curves wherein actually computed values of maxima occur close to the r_0/x_0, y_0 limiting line. This reduces any extrapolation or interpolation error. The dispersion of apex point a, q values for $\xi_0 = 0$ and $\xi_0 = \pi$ in Table 1 shows, for cases which are identical insofar as the mass spectrometer operation is concerned, the extent of computational as well as data processing error for two initial phases differing by 2π radians.

DISCUSSION

There exists no a priori reason to expect that the practical stability diagrams will remain confined within the conventional stability diagram. That this is indeed realized in practice, is shown by the practical stability diagrams occurring beyond the confines of the stability diagram representing the qualitative solution of Mathieu's equation. The shift pattern of the apex points on the a, q plane as a function of the initial velocity–position–phase conditions is complex. While a detailed qualitative correlation involving all the initial conditions is difficult, an explanation of movement of the limit lines with entry phase seems possible. It can be seen from Fig. 2 as well as from the results given in Table I that the x limit lines move out farthest around $\xi_0 = 3\pi/4$ and move in closest around $\xi_0 = \pi/4$ while for the y limit lines the opposite is true. This correlates reasonably to the entry phase electrode potential and its immediate trend of change with ξ, since, in the x direction the potential is expected to be most strongly focusing for ions around $\xi_0 = 3\pi/4$ and most weakly focusing around $\xi_0 = \pi/4$; in the y direction, the potential is expected to be most strongly defocusing around $\xi_0 = 3\pi/4$ and most weakly defocusing around $\xi_0 = \pi/4$.

It is clear from Figs. 1 and 2 that the practical stability diagrams will shift, depending on the initial conditions of velocity and position as well as on the phase at injection. Since the mass filter resolution depends on the interval Δq in the region of stability on the constant a/q line, the resolution for specific initial ion injection conditions will depend on the location of the practical stability diagram apex point on the a, q plane and hence on the specific initial condition used. The resolution therefore will not be uniquely specified by the a/q ratio but will vary, depending on the initial conditions, and thus the same constant a/q line will correspond to low resolutions for some initial conditions and at the same time that of infinite resolution (i.e., if it goes through the peak of any practical stability diagram) for some other set of initial conditions. It is also obvious from Fig. 1 that at constant a, increase in the q of the apex point implies higher resolution, and for constant q, an increase in a of the apex point implies lower resolution, both for a constant a/q line of operation. The definition of resolution used by Paul et al. [1, 3] makes use of a, q values of the apex of the conventional stability diagram. Since the x, y limit lines of the practical stability diagrams are parallel to the corresponding limit lines of the conventional stability diagram, one can, on the basis of the slopes of these lines, write

$$\frac{m}{\Delta m} = \frac{q_{\text{apex}}}{\Delta q} = \frac{(0.623\, q_{\text{apex}} - a_{q_{\text{apex}}})(1.246\, q_{\text{apex}} + a_{q_{\text{apex}}})}{1.869\, q_{\text{apex}}(a_{\text{apex}} - a_{q_{\text{apex}}})}$$

where q_{apex} and a_{apex} define the apex point of a practical stability diagram, and $a_{q_{\text{apex}}}$ represents the a value a constant a/q line takes at q_{apex}. The variation of q_{apex} and $a_{q_{\text{apex}}}$ in the a, q region investigated has little effect on $m/\Delta m$ owing to

the terms in the numerator. Thus, on the basis of an assumption of average values of q_{apex} and $a_{q_{apex}}$, one obtains $m/\Delta m = 0.178/(a_{apex} - a_{q_{apex}})$ for an expression of resolution which can be applied to individual practical diagrams. For a set of specific values of x_0, x_0', y_0, y_0' and ξ_0, the ions can only be either bounded or beyond the bounds, corresponding to a hundred or zero percent transmission respectively. As a consequence, the resulting mass peaks should be rectangular in such a mode of injection.

The general feature of the locus of practical stability diagram apex points, as shown in Fig. 2, is a closed cycle from $2\xi_0 = 0$ to $2\xi_0 = 2\pi$. The pattern remains essentially the same for all the initial conditions investigated. The observation that, for the beginning of the phase cycle, the q values are relatively smaller is of a general nature. It should be pointed out that, for a given constant a/q line cutting across the practical stability diagram apex point locus, all those phases for which the peak points fall below the intersecting line imply that the ion will be lost when entry at the corresponding phases takes place. Those entry phases for which the peak points are above the line contribute to transmission trajectories. Also, the larger the total Δq intercept of the peak point locus, the poorer will be the resolution for a given radial velocity–position injection. In fact, in such cases there seems to be merit in operating the filter part of the phase cycle so as to keep only a small portion of the apex locus above the constant a/q line. The overall effect, when x_0, x_0', y_0, y_0' also vary, will depend on the energy distribution and injection points of the initial ion sample. The parallelism of the practical stability diagram limit lines with the limit lines of the conventional stability diagrams indicates a relationship of β_x (or β_y) with x_0/r_0, x_0'/r_0 (or y_0/r_0, y_0'/r_0) and ξ_0. In

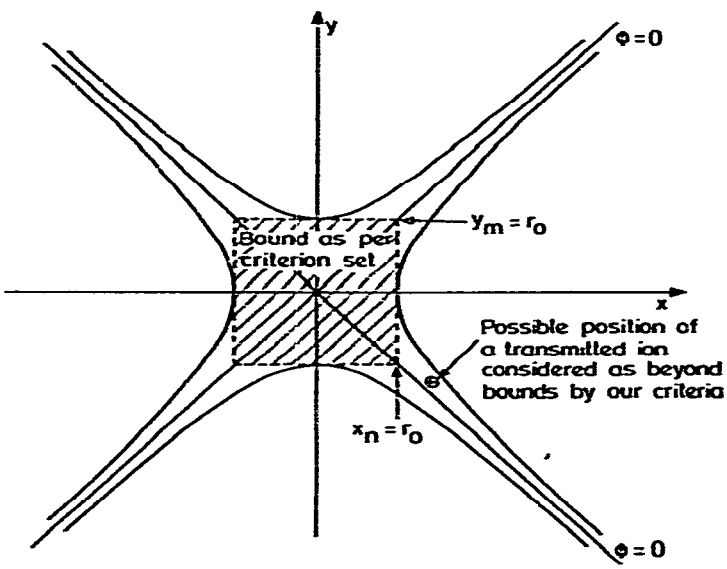

Fig. 3. Criterion used for upper bound of trajectories.

principle, these two quantitative relationships can evolve from Table 1, from which any practical stability diagram, and the apex point locus for the entire phase cycle, can be generated.

One of the limitations of the present set of calculations is the criterion used for arriving at parameter limits for bounded oscillations by considering only those trajectories which go beyond the bound of field dimension in either the x or y direction independently, and no attempt has been made to consider both amplitudes simultaneously (Fig. 3). This should have been done, as those ions, which have both x and y values higher than the imposed bound, i.e., between the hyperbolic rods near the zero potential lines, are not fully taken into account. However, calculations show that the conditions for which the x amplitudes are very large, the y amplitudes are very small, and vice versa [2]. This means that if the ion has an amplitude too high in one direction, it is also close to the same axis, and the criterion used for arriving at the parameter limits for bounded oscillations has inherently negligible error.

NOTE ADDED IN PROOF

Since submission of this paper, there have been comments in the literature (*Int. J. Mass Spectrom. Ion Phys.*, 14 (1974) 317) about the limiting values reported in our earlier work. Recently, Arvind Arora of this laboratory checked our results using an entirely different computer program calculating up to 160–200 cycles of ion motion. A check of the results for injection conditions 0.01, 0.01; 0.008, 0.008 using all the ξ_0 values and also those for $\xi_0 = 3\pi/8$ using all the initial conditions, show that most of the apex points reported here are within the specified error limits.

REFERENCES

1 W. Paul, H. P. Reinhard and U. von Zahn, *Z. Phys.*, 152 (1958) 143.
2 R. Nagarajan and P. K. Ghosh, *Int. J. Mass Spectrom. Ion Phys.*, 12 (1973) 79; 14 (1974) 267.
3 W. Paul and M. Raether, *Z. Phys.*, 140 (1955) 262.